Acknowledgments

We gratefully acknowledge the typographical assistance of Helen Bell.

References

Agrawal, B. B. L., & Goldstein, I. J. (1967) *Biochim. Biophys. Acta 147*, 262.
Ash, J. F., & Singer, S. J. (1976) *Proc. Natl. Acad. Sci. U.S.A. 73*, 4575.
Axelrod, D., Koppel, D. E., Schlessinger, J., Elson, E. L., & Webb, W. W. (1976) *Biophys. J. 16*, 1055.
Barbarese, E., Sauerwein, H., & Simkins, H. (1973) *J. Membr. Biol. 13*, 129.
Brownlee, K. A. (1965) *Statistical Theory and Methodology in Science and Engineering*, pp 299, 560, Wiley, New York.
Burleson, G. R., Kulpa, C. F., Edwards, H. E., & Thomas, J. K. (1978) *Exp. Cell Res. 116*, 298.
Burridge, K. (1976) *Proc. Natl. Acad. Sci. U.S.A. 73*, 4457.
Edidin, M., & Weiss, A. (1974) in *Control of Proliferation in Animal Cells* (Clarkson, B., & Basarga, R., Eds.) p 213, Cold Spring Harbor Laboratory, Cold Spring Harbor, NY.
Edwards, H. E., Thomas, J. K., Burleson, G. R., & Kulpa, C. F. (1976) *Biochim. Biophys. Acta 448*, 541.
Fahey, P. F., & Webb, W. W. (1978) *Biochemistry 17*, 3046.
Fernandez, S. M., & Berlin, R. D. (1976) *Nature (London) 264*, 411.
Gaffney, B. J. (1975) *Proc. Natl. Acad. Sci. U.S.A. 72*, 664.
Gunther, C., Wang, J. L., Yahara, I., Cunningham, B. A., & Edelman, G. M. (1973) *Proc. Natl. Acad. Sci. U.S.A. 70*, 1012.
Hatten, M. E., Scandella, C. J., Horwitz, A. F., & Burger, M. M. (1978) *J. Biol. Chem. 253*, 1972.
Inbar, M., Shinitzky, M., & Sachs, L. (1973) *J. Mol. Biol. 81*, 245.
Jacobson, K., Wu, E.-S., & Poste, G. (1976) *Biochim. Biophys. Acta 433*, 215.
Jainchill, J. L., & Todaro, G. J. (1970) *Exp. Cell Res. 59*, 137.
Kosower, N. S., Kosower, E. M., Lustig, S., & Pluznik, D. H. (1978) *Biochim. Biophys. Acta 507*, 128–136.
Lee, N., & Scandella, C. (1979) *J. Supramol. Struct., Suppl. 3*, 191.
Maeda, T., Eldridge, C., Toyama, S., Ohnishi, S., Elson, E. L., & Webb, W. W. (1979) *Exp. Cell Res. 123*, 333.
McPherson, I. (1969) in *Fundamental Techniques in Virology* (Habel, K., & Salzman, N. P., Eds.) p 214, Academic Press, New York.
Nicolau, C., Hildebrand, K., Beimann, A., Johnson, S. M., Vaheri, A., & Frids, R. R. (1978) *Exp. Cell Res. 113*, 63.
Nicolson, G. L. (1974) in *Control of Proliferation in Animal Cells* (Clarkson, B., & Basarga, R. Eds.) p 251, Cold Spring Harbor Laboratory, Cold Spring Harbor, NY.
Nicolson, G. L. (1976) *Biochim. Biophys. Acta 458*, 1.
Pollack, R., Osborn, M., & Weber, K. (1975) *Proc. Natl. Acad. Sci. U.S.A. 72*, 994.
Rosenblith, J. Z., Ukena, T. E., Yin, H. H., Berlin, R. D., & Karnovsky, M. J. (1973) *Proc. Natl. Acad. Sci. U.S.A. 70*, 1624.
Rutishauser, U., & Sachs, L. (1974) *Proc. Natl. Acad. Sci. U.S.A. 71*, 2456.
Rutishauser, U., Sachs, L., Yahara, I., & Edelman, G. M. (1974) *Proc. Natl. Acad. Sci. U.S.A. 71*, 1149.
Schlessinger, J., Koppel, D. E., Axelrod, D., Jacobson, K., Webb, W. W., & Elson, E. L. (1976) *Proc. Natl. Acad. Sci. U.S.A. 73*, 2409.
Schlessinger, J., Axelrod, D., Koppel, D. E., Webb, W. W., & Elson, E. L. (1977a) *Science 195*, 307.
Schlessinger, J., Elson, E. L., Webb, W. W., Yahara, I., Rutishauser, U., & Edelman, G. M. (1977b) *Proc. Natl. Acad. Sci. U.S.A. 74*, 1110.
Todaro, G. (1969) in *Fundamental Techniques in Virology* (Habel, K., & Salzman, N. P., Eds.) p 220, Academic Press, New York.
Wolf, D. E. (1978) Ph.D. Thesis, Cornell University.
Wolf, D. E., Schlessinger, J., Elson, E. L., Webb, W. W., Blumenthal, R., & Henkart, P. (1977) *Biochemistry 16*, 3476.

Effect of Ethidium Bromide on Deoxyribonucleic Acid Internal Motions†

Michael E. Hogan* and Oleg Jardetzky

ABSTRACT: We have used ^{31}P and ^{1}H NMR to show that DNA internal motions are stopped or greatly hindered when ethidium bromide intercalates into DNA. We show that the effect is localized to a 2 base pair long DNA region at the binding site and that internal motions outside the binding site are nearly unaffected. Based upon the nearly independent behavior of bound and free DNA regions, we conclude that in B-DNA individual base pairs experience internal motion which is independent of the motion of their neighbors.

Recent nuclear magnetic resonance studies of long DNA[1] fragments have shown that the internal structure of B-form DNA is not rigid but instead experiences large fluctuations in nucleotide conformation which occur with a time constant near 10^{-9} s (Hogan & Jardetzky, 1979; Bolton & James, 1980; Klevan et al., 1979; Early & Kearns, 1979).

Based upon ^{31}P NMR relaxation measurements, Klevan et al. (1979) have shown that the backbone phosphates of DNA

† From the Stanford Magnetic Resonance Laboratory, Stanford University, Stanford, California 94305. *Received December 11, 1979.* This research was supported by grants from the National Institutes of Health (RR00711) and the National Science Foundation (GP23633 and PCM78-07930). M.E.H. is a Fellow in Cancer Research supported by DR 6-283-F of the Damon Runyon–Walter Winchell Cancer Fund.

[1] Abbreviations used: ^{13}C, carbon-13; DNA, deoxyribonucleic acid; EB, ethidium bromide; ^{1}H, proton; NMR, nuclear magnetic resonance; ^{31}P, phosphorus-31.

0006-2960/80/0419-2079$01.00/0

experience a large fast motion inside the helix which occurs with a calculated time constant near 0.5×10^{-9} s. Both of the above groups of authors have suggested that fast phosphate motions are due to rotations about phosphate–oxygen bonds ω and ω'. As has been stated (Klevan et al., 1979), such rotation will produce only small displacements of the two nucleosides adjoining phosphate in the helix.

However, as has been shown from ^{1}H line width measurements of the exchangeable base-paired protons in DNA (Early & Kearns, 1979) and from ^{1}H and ^{13}C NMR relaxation measurements (Hogan & Jardetzky, 1979, and unpublished experiments), the B-DNA helix must experience large fluctuations in the conformation of the base and sugar as well as the deoxyribose–phosphate backbone. The lines of the ^{1}H, ^{31}P, and ^{13}C spectra of the base and sugars are too narrow to be due to overall motion alone.

Our best fit of ^{1}H, ^{13}C, and ^{31}P NMR relaxation times to a two-state model predicts substantial fluctuations about a geometry near that of a B-DNA helix; position C_2 of the deoxyribose sugar, ±35°; the base planes, ±20°; the phosphate–proton vectors in the backbone, ±25°. Within the accuracy of the model, the time constants for these internal motions are the same, between 1×10^{-9} and 2×10^{-9} s (Hogan & Jardetzky, 1979, and unpublished experiments).

On the basis of these findings, we have proposed a working hypothesis which predicts that the base plane motion which we monitor must arise from the motion of the C_2 axis (the short axis of the base planes in the helix). We propose that at the same time, deoxyribose sugar pucker geometry fluctuates inside the helix with a time constant near 10^{-9} s. That rapid change in sugar conformation necessarily changes the geometry of the sugar–phosphate backbone. Because they are coupled in this way, the time constants measured at phosphate and in the sugar are nearly the same.

It should be noted that the correlation time which we have calculated for phosphorus in DNA, 2.2×10^{-9} s (Hogan & Jardetzky, 1979, and unpublished experiments), differs by a factor of 4 from that calculated by Bolton & James (1980) or by Klevan et al. (1979) This difference, although small in a qualitative sense, is greater than expected from differences in the models used for calculating motions and is due, we believe, to differences in measured ^{31}P–{^{1}H} NOE values; Klevan et al. have measured NOE = 1.6 for 140 base pair long DNA, Bolton and James, 1.56 for sonicated DNA of unspecified length; Hogan and Jardetzky, 1.35 for 140 base pair long DNA and 1.38 for 260 base pair long DNA (Hogan and Jardetzky, unpublished experiments). We cannot offer an explanation for these differences at this time.

On the other hand, the correlation time which we have measured for the internal motion of the DNA base planes from ^{13}C NMR relaxation measurements (1×10^{-9} s) is *faster* than the effective correlation time (3×10^{-7} s) calculated by Early & Kearns (1979) from line widths of hydrogen-bonded imino protons. It must be stated, however, that the Early & Kearns (1979) calculations are only a rough approximation. The calculated value (3×10^{-7} s) refers to a correlation time for the unrestricted motion of a rigid DNA segment that is small enough to have imino resonances as narrow as the measured values. To be precise, the Early & Kearns (1979) model specifies that long DNA helixes have line widths as narrow as those expected for a free, rigid 70 base pair long rod. Long DNA helixes do not behave as unlinked 70 base pair long segments; therefore, the effective rodlike correlation time calculated by Early & Kearns (1979) must be a weighted average of both slow overall and fast internal motions, but the rates or the relative contributions of these motions cannot be determined from proton line widths only. It is, however, interesting to note that if both proton and nitrogen relaxation mechanisms are taken into account, the measured imino proton line widths are completely consistent with the rate and amplitude of base plane motion which we have calculated from ^{13}C NMR.

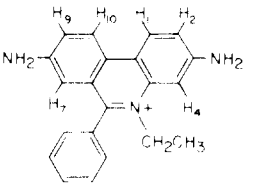

FIGURE 1: Structure of ethidium bromide.

To appreciate fully the effect of such motions on the NMR properties of DNA, it is necessary to consider exactly what would happen if these motions were stopped. During times shorter than 10^{-4} s, the long axis of a 300 base pair long DNA helix (L = 1200 Å) moves in solution as if it were a rod with a time constant for that motion near 10^{-5} s (Hogan et al., 1978). Using standard relationships (Woessner, 1962), we calculate that in a rigid 300 base pair long helix the line widths of backbone phosphates and of most nucleotide protons would be $\gg$10 s.

If T_1 values or line widths were of this order of magnitude, resonances could not be detected by ordinary NMR pulse sequences. Therefore, ^{13}C, ^{1}H, and ^{31}P NMR spectra can be measured in long DNA helixes *only* because nucleotides in the helix experience conformational fluctuations near 10^{-9} s with amplitudes greater than ±20°

The geometric constraints placed upon DNA when ligands bind to the helix make it likely that large DNA internal motions will be severely hindered in a tight DNA–ligand complex. If, due to ligand binding, the amplitude of DNA motions were reduced or if the rate of the motions were made significantly slower, then DNA regions at the binding site would behave as if they were rigid; i.e., ^{31}P or ^{1}H NMR spectra of bound DNA regions would then become unmeasurable in solution.

In the present study using ^{31}P and ^{1}H NMR, we have measured DNA area and relaxation time changes which occur when the intercalating drug ethidium bromide (EB, Figure 1) binds to a 300 base pair long DNA fragment. We find that when EB binds to DNA, ^{1}H and ^{31}P NMR resonance area becomes unmeasurable within a 2 base pair long region. We also find that the relaxation properties of DNA outside the binding site are nearly unaffected by bound EB. From these observations, we conclude that base plane and deoxyribose and phosphate backbone internal motions are "frozen out" within the 2 base pair long EB–DNA complex but that DNA regions immediately adjacent to the complex are nearly unaffected.

Experimental Procedures

Calf thymus DNA (Miles Laboratories) was S1 nuclease digested, deproteinized, and fractionated by length as previously described (Hogan & Jardetzky, 1979). The DNA used in this work has been sized on 5% polyacrylamide gels relative to the *Hae*III restriction fragments of ϕX 174 (New England Biolabs). The average length of the material is 300 base pairs; more than 75% of the material has a length within 50 base pairs of that average value. Relative to the *Hae*III markers, the material had identical mobility on denaturing 7 M urea gels, which implies that it is free from nicks or terminal single-stranded regions. The DNA was also digested analytically

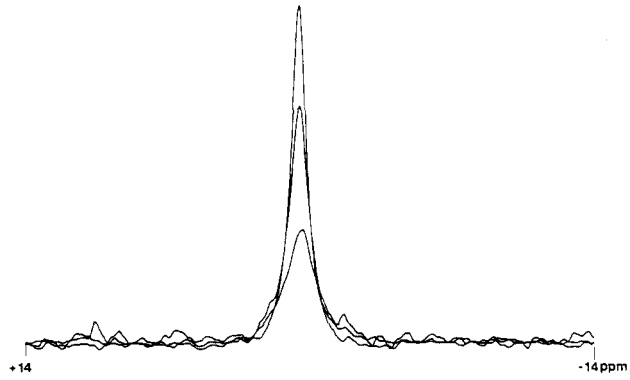

FIGURE 2: Effect of ethidium bromide binding on the ^{31}P NMR spectrum of 300 base pair long DNA. Samples are in 30 mM Tris, 3 mM Na_2EDTA, pH 7.2, and D_2O. Fourier transform spectra were accumulated with quadrature detection at 40.511 MHz on a modified Varian XL100 spectrometer equipped with a Nicolet multiple nuclei accessory. Spectra were collected with nonselective proton decoupling, acquisition time 1.7 s, with a delay between pulses of 5 times the measured ^{31}P T_1 value. Chemical shifts are referenced to an external standard (85% H_3PO_4–15% D_2O). Temperature was controlled at +23 °C. DNA concentration was 6.7×10^{-3} M (base pairs/liter). (Top) $r_{ad} = 0$, 16-s delay between pulses, 2000 transients; (middle) $r_{ad} = 0.1$, 18-s delay, 2000 transients; (bottom) $r_{ad} = 0.3$, 30-s delay 2000 transients.

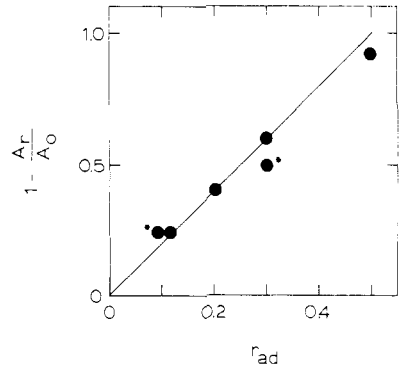

FIGURE 3: Effect of EB binding on ^{31}P NMR area. ^{31}P spectra were accumulated in 30 mM Tris, 3 mM EDTA, pH 7.2, and D_2O as specified in Figure 2. The data presented for each r_{ad} value are the average of three independent area determinations. (●) 6.7 mM, 2000 transients; (●*) 3.35 mM, 4000 transients.

under standard conditions (Hogan & Jardetzky, 1979) with S1 nuclease (Sigma Chemical Co.) and was found to contain 2 ± 2% of S1 nuclease digestible material, confirming that the DNA is free from single-stranded contamination. DNA concentration was determined optically by using $\epsilon_{258} = 1.29 \times 10^4$ cm^{-1} M^{-1} (measured in base pairs).

Ethidium bromide (Sigma Chemical Co.) was repurified by recrystallation from 1-butanol. The concentration was determined optically by using $\epsilon_{483} = 5350$ cm^{-1} M^{-1}.

NMR titrations were performed by the direct addition of EB in the appropriate buffer to DNA solutions. In all instances, volume corrections were less than 5%.

Results

Phosphorus-31 Nuclear Magnetic Resonance. In Figure 2 is shown the effect of EB binding on the ^{31}P NMR spectrum of 300 base pair long DNA. Chemical shifts are not affected by binding; however, the area of the phosphate resonance is greatly reduced. In all cases, spectra have been accumulated with a delay between acquisitions which was 5 times greater than the measured T_1 value of the complex; a delay of 10 times T_1 produced no additional intensity changes (data not shown). Consequently, the decrease in ^{31}P area measured here must arise either from a major broadening of some phosphate resonances in the EB–DNA complex or from an increase in the T_1 relaxation time of some resonances to a value greater than 30 s.

EB-induced changes in the area of the phosphorus resonance band have been quantified and are plotted in Figure 3 as a function of the ratio of added EB to total base pairs (r_{ad}). EB binds tightly to DNA in the low salt buffers used here, $K_B > 10^6$ M^{-1} (LePecq & Paoletti, 1967). Consequently, at the DNA concentrations used, binding is nearly quantitative at all r_{ad} values below EB binding saturation and is therefore not affected by increased DNA concentration, as seen in Figure 3.

Data are presented as $1 - (A_r/A_0)$ vs. r_{ad}, where A_r is the resonance area measured at a value r_{ad} and A_0 is the area in the absence of EB. When plotted in this way, the reduction of ^{31}P area will be linear if the number of phosphates affected by EB binding is independent of the degree of saturation, i.e., if EB binding measured by ^{31}P is noncooperative.

The maximum value of $1 - (A_r/A_0)$ reached at high r_{ad} values corresponds to that fraction P of ^{31}P resonance area which can be lost in the saturated EB complex. If binding is noncooperative, the intersection of that maximum value and a linear fit to the low r_{ad} value data corresponds to $1/n$, where n equals the number of base pair equivalents lost for each bound EB molecule. If linear, a fit of the low r_{ad} value data yields a slope m where $m = Pn$.

As seen in Figure 3, low r_{ad} value ^{31}P NMR data are well fit by a straight line with the slope $m = 1.9 \pm 0.2$. This suggests that the EB-induced decrease in ^{31}P area is not cooperative. At high r_{ad} values, the entire ^{31}P signal from DNA is lost ($P = 1$), meaning that every phosphate in DNA is sensitive to EB binding.

Together, the data suggest that regardless of the degree of saturation, an area contribution corresponding to four DNA phosphates is lost for each EB bound to DNA ($m \simeq n \simeq 2$). The intercalated EB complex covers 2 base pairs (Bauer & Vinograd, 1970). Therefore, we propose that those four phosphates which become unmeasurable due to EB binding are localized within the EB binding site.

Proton Nuclear Magnetic Resonance. As we have suggested, the internal motion of a deoxyribose sugar should be strongly coupled to motions of the sugar–phosphate backbone in a DNA helix (Hogan & Jardetzky, 1979). If DNA internal motions are hindered in the backbone of the helix, then we expect that motion monitored in the sugar should be affected as well.

A ^1H NMR spectrum of free 300 base pair long DNA is shown in Figure 4 (upper traces). We have assigned band I to base protons H_8, H_6, and H_2; the downfield shoulder at 7.9 ppm is almost certainly from H_8 (Hogan & Jardetzky, 1979). Band II is assigned to cytosine base proton H_5 and to the glycosidic protons $H_{1'}$. Band IV is assigned to deoxyribose protons $H_{3'}$, $H_{4'}$, and $H_{5'}$ as a group; band V is assigned to protons $H_{2'}$; band VI is assigned to thymidine methyl group protons. The areas of the resonances do not increase upon melting, suggesting that nearly every nucleotide in the helix contributes to the spectrum (Hogan & Jardetzky, 1979).

In all B-type DNA helixes, base protons H_8, H_6, and H_5 and all deoxyribose protons have proton neighbors closer than 3 Å (Arnott et al., 1969). If nucleotides were fixed rigidly in a 300 base pair long helix, then dipolar interactions between protons would increase the T_1 values of these protons to $\gg 10$ s and make these proton resonances several kilohertz wide (Woessner, 1962), too broad to be measured in solution.

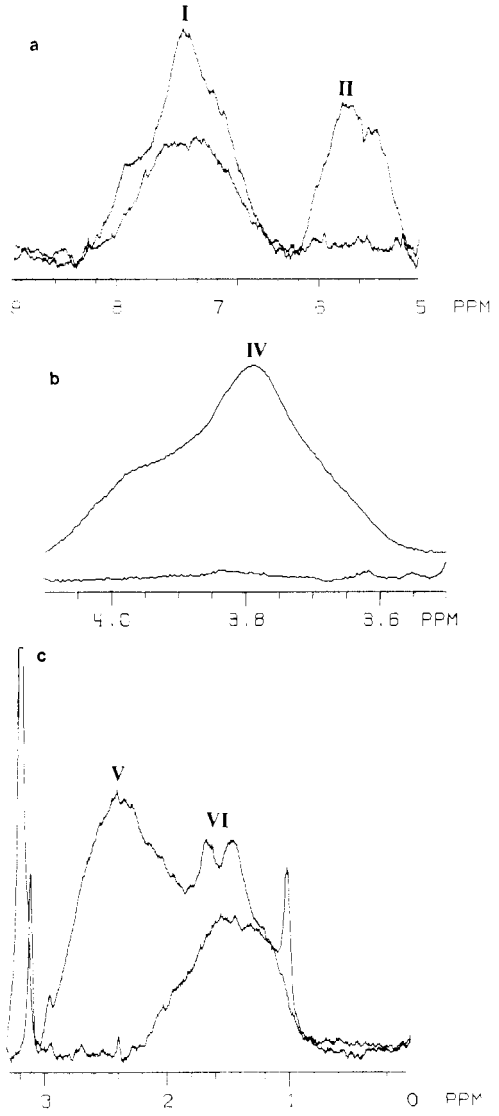

FIGURE 4: Effect of EB binding on the nonexchangeable proton spectrum of 300 base pair long DNA. Fourier transform spectra were accumulated with quadrature detection on a Bruker HXS-360 spectrometer with a 0.8-s acquisition time and a 10-s delay; 400 transients have been averaged per spectrum. Chemical shifts are referenced with respect to external Me_4Si. DNA concentration was 4.7 mM in 20 mM NaCl, 7 mM Na_2HPO_4, 2 mM NaH_2PO_4, 1 mM Na_2EDTA, pH 7.2, and D_2O. Temperature was controlled at +23 °C. (Top spectrum) $r_{ad} = 0$; (bottom spectrum) $r_{ad} = 0.53$.

On the other hand, adenine protons H_2 may have relatively small proton line widths and T_1 values even in the absence of DNA internal motion. In deuterated buffers, the proton neighbor closest to H_2 in a B-DNA helix is another H_2 proton on an adjacent AT base pair, greater than 3.4 Å away (Arnott et al., 1969). The closest proton neighbor within the nucleotide is the $H_{1'}$ sugar proton 4.5 Å away (Arnott et al., 1969). At these distances, intramolecular dipole relaxation between protons is weak. Therefore, other relaxation processes, such as those with solvent, may contribute significantly to the line width and T_1 value of H_2 proton resonances in DNA (Woessner, 1962). Solvent interactions with H_2 occur on the surface of the helix and may not be significantly altered upon binding EB. Consequently, if line widths and T_1 values are sufficiently small so that H_2 protons can be measured in free DNA, then the H_2 proton spectrum may not change greatly if EB were to stop DNA internal motions.

^1H NMR area changes which occur when EB binds to DNA are shown in Figures 4 and 5. To eliminate buffer contributions, we have accumulated ^1H spectra of DNA samples in a phosphate buffer rather than the Tris-HCl buffer used for ^{31}P NMR (pH and total cation concentration are held constant). Such a change in buffer should have little effect on DNA structure or on the structure of the EB–DNA complex. Data have been collected with a delay time between pulses which was 5 times longer than the longest measured T_1 value in the spectra. As predicted from EB effects on phosphate resonances, ^1H NMR area is lost from several bands when EB binds to DNA. In Figure 5, the low r_{ad} data can in all cases be fit as a straight line saturating at $r_{ad} = 0.5$. The best linear fit of the data yields the following: for band II, $m = 2.2 \pm 0.4$, $n = 2 \pm 0.3$, and $P = 1$; for band IV ($H_{3'}$, $H_{4'}$, and $H_{5'}$), $m = 2.2 \pm 0.5$, $n = 2 \pm 0.5$, and $P = 1$; for band V ($H_{2'}$), $m = 1.7 \pm 0.5$, $n = 1.9 \pm 0.3$, and $P = 1$.

The line drawn through the data for bands II, IV, and V in Figure 5 is that r_{ad} dependence corresponding to an area loss of 2 base pair equivalents per bound EB molecule ($m = n = 2$), which saturates when every base pair in the helix has been affected ($P = 1$). The data fit this model well, which suggested that resonance area from four sugar residues is lost at the EB binding site.

In Figure 5, the contribution of base proton H_5 to band II shows an r_{ad} dependence indistinguishable from that of deoxyribose protons, suggesting that the resonance area from aromatic proton H_5 is also lost within the 4 base pair long binding site. In contrast, the area change measured for band I (H_8, H_6, and H_2) is more complicated. As seen in Figure 5, the area of band I decreases with a slope $m = 1.2 \pm 0.2$, saturating at $r_{ad} = 0.5$ to yield a residual intensity $P = 0.6$; only 60% of band I is sensitive to EB binding. As seen in Figure 4, the unaffected contribution to band I is centered at 7.4 ppm (as expected for H_2 protons) and has a T_1 value only slightly different from the average value of band I in free DNA (Table I). The magnitude of the residual contribution to band I (40%) is ~20% greater than that expected for H_2 from the base composition of calf thymus DNA (Marmur & Doty, 1962). During preparation, the DNA samples used here have been exhaustively dialyzed against deuterated buffers. During that dialysis, it is expected that a significant fraction of H_8 protons exchange for deuterium (Schweizer et al., 1964), increasing the relative contribution of H_2 protons to band I. Therefore, we assign the residual proton resonance area at 7.4 ppm to aromatic proton H_2 and that area in band I which is sensitive to EB to protons H_8 and H_6. As seen in Figure 5, the r_{ad} dependence of the loss of H_8 and H_6 resonance area ($m/P \simeq n \simeq 2$) is identical with that value measured for other protons in DNA, suggesting that the contribution of aromatic protons H_8 and H_6 is also lost within the EB binding site.

Exchangeable DNA Base-Paired Resonances. Figures 5c and 6 show the change in the area of hydrogen-bonded DNA resonances which occurs when EB binds to 300 base pair long DNA. Spectra have been accumulated in H_2O by using a Redfield-type long pulse (Redfield & Kunz, 1975). In all cases, a delay between acquisitions was used which was sufficiently long so that additional increases in the delay failed to increase the resonance area.

The band at 13.5 ppm in Figure 6 corresponds to the thymine N_3 proton of AT base pairs and that at 12.4 ppm corresponds to the guanine N_1 proton of GC base pairs (Early & Kearns, 1979). As was seen for phosphates and for the nonexchangeable protons, the hydrogen-bonded resonance area becomes unmeasurable when EB binds to DNA (Figure 6). The r_{ad} dependence of the total EB-induced area change (AT

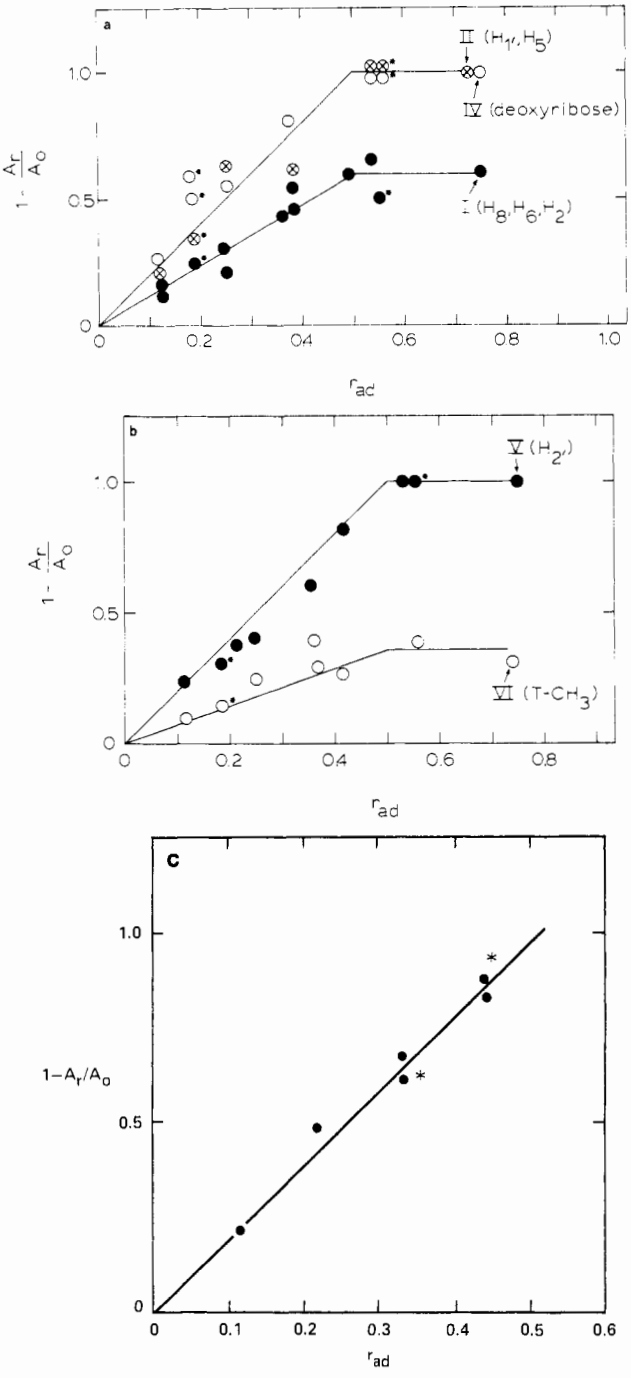

FIGURE 5: Effect of EB binding on ^1H NMR area. In (a) and (b), spectra have been accumulated in 20 mM NaCl, 7 mM NaH_2PO_4, 2 mM Na_2HPO_4, 1 mM EDTA, pH 7.2, and D_2O, as specified in Figure 4. In (c), spectra have been accumulated as in Figure 6. In (a) and (b), areas have been estimated from peak heights. Areas listed in (c) correspond to the full integrated area of AT + GC hydrogen-bonded resonances. a: (●) band I, 4.7 mM; (●*) band I, 2.35 mM; (⊗) band II, 4.7 mM; (⊗*) band II, 2.35 mM; (○) band IV, 4.7 mM; (○*) band IV, 2.35 mM. b: (●) band V, 4.7 mM; (●*) band V, 2.35 mM; (○) band VI, 4.7 mM; (○*) band VI, 2.35 mM. c: (●) exchangeable resonances, 17.6 mM; (●*) exchangeable resonances, 8.9 mM.

+ GC base pairs) has been quantified and is plotted in Figure 5c. The data suggest that every base pair in the helix is affected at EB binding saturation ($P = 1$). The best linear fit of the data gives a slope $m = 2.0 \pm 0.2$ and $n = 2 \pm 0.3$, implying that, independent of base composition, the hydrogen bonds in 2 base pairs become unmeasurable at the EB binding site.

Table I[a]

Phosphorus-31 Nuclear Magnetic Resonance			
r_{ad}	T_1 (s)	T_2 (ms)	$\Delta\nu$
0	3.5 ± 0.2	16 ± 2.5	35 ± 3
0.1	3.6 ± 0.2	10 ± 2.0	50 ± 5
0.2	5.0 ± 1	4 ± 0.5	65 ± 10
0.3	6.0 ± 2	4 ± 0.5	90 ± 10

Proton Nuclear Magnetic Resonance				
	T_1(I or II)		T_1(VI or V)	
r_{ad}	(s)	$\Delta\nu$	(s)	$\Delta\nu$
0[b]	1.6 ± 0.1[b]	250[b]	0.9 ± 0.1[d]	50[d]
0.53[b]	2.4 ± 0.3[b]	350[b]	1.7 ± 0.2[d]	100[d]
0[c]	1.3 ± 0.2[c]	220[c]	0.9 ± 0.2[e]	270[e]
0.18[c]	1.3 ± 0.3[c]	250[c]	1.3 ± 0.3[e]	270[e]
0.36[c]	1.5 ± 0.4[c]	300[c]	1.0 ± 0.3[e]	300[e]

[a] T_1 measurements for ^{31}P and ^1H NMR were made by using a standard inversion recovery sequence. T_2 measurements were made by using the Hahn–Spin echo sequence. Line widths ($\Delta\nu$) were measured directly from bandwidths at half-height and are therefore not corrected for chemical shift heterogeneity. Errors reported for T_1 and T_2 are twice the standard deviation of a linear least-squares fitting of the data. Sample conditions are as specified in the legends to Figures 2 and 4. [b] For band I. [c] For band II. [d] For band VI. [e] For band V.

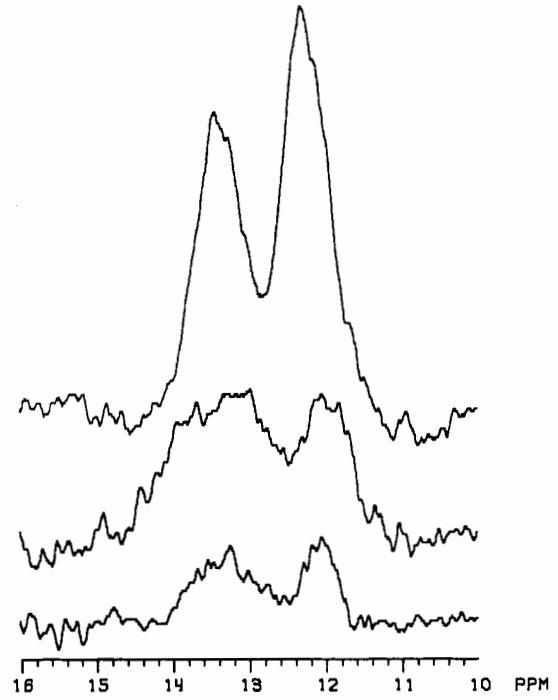

FIGURE 6: Effect of EB on the exchangeable proton spectrum of 300 base pair long DNA. Spectra were accumulated by using the Redfield 214 pulse sequence (Redfield & Kunz, 1975) with quadrature detection on a Bruker HXS-360 spectrometer. Pulse length ($10 \times P_2$) = 370 μs; spectral offset from water = 2628 Hz; 3-s delay between acquisitions; 500 acquisitions per spectrum. DNA concentration was 8.9 mM (base pairs) in 20 mM NaCl, 7 mM NaH_2PO_4, 2 mM Na_2HPO_4, 1 mM Na_2EDTA, and H_2O, pH 7.2; temperature was controlled at +23 °C. Chemical shifts are referenced with respect to external Me_4Si. (Top) $r_{ad} = 0$; (middle) $r_{ad} = 0.22$; (bottom) $r_{ad} = 0.44$.

EB Side-Chain Motion and Thymidine Methyl Group Rotation Continue in the DNA Complex. Both the EB methyl resonance (1.1 ppm) and the thymidine methyl resonance (1.4 ppm) can be measured in the saturated EB–DNA complex (Figure 4). The EB methyl group is part of a flexible ethyl side group and as a result can move independently of the rest of the molecule. When intercalated, the ethyl side group faces outward from the small DNA groove, appearing in the

available crystal structures to be nearly unhindered by contacts with the helix (Tsai et al., 1975, 1977). The narrowness of the EB methyl resonance measured at EB binding saturation confirms that the side group is free to move in the small groove.

The thymidine methyl group projects into the large DNA groove and there is capable of fast rotational motion about the C_5–CH_3 bond. The time scale for such methyl rotation in small molecules is typically 10^{-9}–10^{-12} s (Andrew et al., 1974). If rotation occurred at that rate in the helix, it could produce, in free DNA, the small line widths and T_1 values measured for thymidine methyl resonances, independent of other motions inside the helix (Woessner, 1962; King & Jardetzky, 1978).

As seen in Table I and Figure 4, the line width and T_1 value of the thymidine methyl resonance are only weakly affected by EB binding. This suggests that thymidine methyl group rotation is unhindered in the EB–DNA complex, no doubt because it faces into the large DNA groove, away from bound EB (Arnott et al., 1969).

Discussion

Internal Motion Is Lost within the EB Binding Site. Here, we have shown that within a 2 base pair long DNA region, resonance area from protons H_8, H_6, and H_5, from deoxyribose protons, and from the Watson–Crick hydrogen-bonded protons is lost simultaneously when EB intercalates into DNA. The simplest interpretation of this area loss is that internal motion of both the base planes and the deoxyribose sugar is greatly hindered within the 2 base pairs adjacent to intercalated ethidium bromide.

The stoichiometry of phosphorus area loss is more complicated, but is due, we believe, to the coupling which exists between phosphorus and deoxyribose motions. In a B-type helix, the average orientation of the P–$H_{3'}$ vector (θ) is near 55° with respect to the long helix axis, while the two P–$H_{5'}$ vectors are more nearly perpendicular to the long axis (Arnott et al., 1969). In a rod, dipolar relaxation is weighted by the squared cosine of θ: $3\cos^2\theta - 1$ (Woessner, 1962). For $\theta \approx 54°$, this term is very small; therefore, in a B helix the motion of the two P–$H_{5'}$ vectors will contribute *more* than two-thirds of P–H dipolar relaxation; to a good approximation, backbone phosphate motion monitored by ^{31}P NMR will be determined exclusively by the motion of the P–$H_{5'}$ vectors.

Earlier, we proposed that the internal motion monitored by phosphate was caused by fast fluctuations of deoxyribose sugar puckering that gave rise to fluctuations in P–$H_{3'}$ and P–$H_{5'}$ vectors (Hogan & Jardetzky, 1979). That model predicted that if sugar motions were to stop, then motion monitored by phosphate must stop as well. Here, ^1H NMR measurements have shown clearly that deoxyribose sugar motion is lost within the 2 base pairs adjacent to EB. We conclude that within that domain there are two phosphates at the site of intercalation which no longer experience P–$H_{5'}$ or P–$H_{3'}$ fluctuation (because they are sandwiched between immobilized nucleotides). As a result, they become unmeasurable. At the boundary between bound and unbound DNA regions, there are four other phosphates; two in which P–$H_{3'}$ motion is hindered (the 3′-phosphates) and two with hindered P–$H_{5'}$ motions (5′-phosphates). Because P–H dipolar relaxation is dominated by motion of the P–$H_{5'}$ vectors, we suggest that the two phosphates at the 5′ end of the complex become unmeasurable when EB binds to DNA. We also conclude that the two phosphates on the 3′ end of the complex (with freely fluctuating P–$H_{5'}$ vectors) are only weakly affected by binding, the result being that EB binding induces a loss of four rather than six DNA phosphate resonances per bound molecule.

Other possible explanations for line broadening or T_1 increases are much less likely. The lifetime of the EB–DNA complex is too long (Bresloff & Crothers, 1975) and the magnitude of the EB-induced chemical shift change is too small (Patel & Canuel, 1976) for chemical exchange broadening to be important to ^{31}P or ^1H NMR relaxation in long DNA helixes. When intercalated, the phenanthridium ring is separated from adjacent nucleotides by ~3–3.4 Å (Tsai et al., 1975, 1977), sufficiently distant that dipolar interaction with adjacent deoxyribose or base protons will be insignificant compared to interactions among protons within the nucleotide.

At the EB binding site, the amine nitrogen and the backbone phosphate are separated in the crystal by 3 Å (Tsai et al., 1975, 1977). At this distance, line broadening due to a scalar interaction with EB nitrogens is unlikely (Abragam, 1961). At the binding site, EB increases base pair separation by 3–3.5 Å (Tsai et al., 1975, 1977). This lengthening could increase the separation between phosphorus and $H_{5'}$ or $H_{3'}$; however, such a lengthening would *decrease* rather than increase line widths or T_1 values in the complex (Woessner, 1962). A decrease in P–H separation is not consistent with the structure of an intercalated EB complex.

Ethidium Is Also Held Rigidly in the Helix. EB has several aromatic resonances which do not overlap with band I (Patel & Canuel, 1976), yet these are not measurable in the complex with 300 base pair long DNA (Figure 5). This implies that the phenanthridium ring of EB is held rigidly in the helix when intercalated. Recently, it has been suggested from fluorescence measurements that EB may wobble in its binding site by ±5° (Wahl et al., 1970). Such wobbling could occur, even though EB resonances cannot be measured in the DNA complex, because, as we have mentioned, 5° motions cannot narrow ^1H lines or shorten the T_1 values of resonances inside a helix 1200 Å long (King & Jardetzky, 1978).

DNA Regions Away from the Binding Site Are Not Affected by EB. The ^{31}P and ^1H relaxation properties of DNA are nearly independent of the level of EB saturation. ^{31}P line widths and T_1 and T_2 relaxation times show the largest increase on binding EB (Figure 2, Table I). However, this increase amounts to only a doubling of T_1 and a fourfold decrease in T_2 at the highest measured r_{ad} value (1 EB bound per 3 base pairs). Much of this measured increase is probably due to the two partially immobilized phosphates at the 3′ end of the EB–DNA complex.

On the other hand, the line widths of exchangeable protons (Figure 6) are nearly independent of EB saturation, as are the line widths and T_1 values of the nonexchangeable protons (Table I) even though 2 base pair equivalents of resonance are lost per bound EB.

Because, in most cases, ^{31}P or ^1H resonances cannot be detected at the binding site, the relaxation properties of the EB–DNA complex are a direct measure of internal motions in unbound DNA regions. Therefore, the insensitivity of these regions to EB binding suggests that DNA internal motions are unaffected outside the 2 base pair long EB binding site.

The inability of bound EB to affect DNA motions at positons beyond its binding site is an important observation because it shows that free internal motion can occur in those nucleotides immediately adjacent to the severely hindered EB complex. Freely mobile and immobile base pairs can coexist in the helix only if the motion of neighboring base pairs is uncorrelated. Therefore, the data presented here suggest that in a B-DNA helix, individual base pairs experience internal motions which are independent of the motions of their neighbors. A corollary of this observation is that bending of

the helix or other long-range cooperative motions of nucleotides cannot be responsible for the DNA motions monitored by NMR.

Loss of DNA Internal Motions May Be Accompanied by DNA Conformational Changes. The most important conclusion to be drawn from the work presented here is that the B-DNA helix does not present itself as a single well-defined structure to a ligand molecule but is instead an averaged structure which is "blurred" by fast internal motions. If, when bound, multiple contacts are made between a ligand and the helix, then internal motions may be obstructed, making the binding site more nearly rigid. Regardless of the details of binding or of the detailed mechanism of internal motion, the process of obstructing DNA motions will necessarily alter the time-averaged conformation of DNA at the binding site; i.e., ligand binding can "freeze" DNA into a rigid conformation substantially different from its averaged conformation in solution.

References

Abragam, A. (1961) *The Principles of Nuclear Magnetism*, pp 308–312, Oxford University Press, London.

Andrew, E. R., Hinshaw, W. S., & Hutchins, M. G. (1974) *J. Magn. Reson. 15*, 196–200.

Arnott, S., Dover, S. D., & Winocott, A. J. (1969) *Acta Crystallogr., Sect. B 25*, 2192–2206.

Bauer, W., & Vinograd, J. (1970) *J. Mol. Biol. 47*, 419–435.

Bolton, P. H., & James, T. L. (1980) *J. Am. Chem. Soc. 102*, 25–31.

Bresloff, J. L., & Crothers, D. M. (1975) *J. Mol. Biol. 95*, 103–123.

Early T. A., & Kearns, D. R. (1979) *Proc. Natl. Acad. Sci. U.S.A. 76*, 4165–4169.

Hogan, M. E., & Jardetzky, O. (1979) *Proc. Natl. Acad. Sci. U.S.A. 76*, 6341–6345.

Hogan, M. E., Dattagupta, N., & Crothers, D. M. (1978) *Proc. Natl. Acad. Sci. U.S.A. 75*, 195–199.

King, R., & Jardetzky, O. (1978) *Chem. Phys. Lett. 55*, 15–23.

Klevan, L., Armitage, I. M., & Crothers, D. M. (1979) *Nucleic Acids Res. 6*, 1607–1616.

LePecq, J. B., & Paoletti, C. (1967) *J. Mol. Biol. 27*, 87–106.

Marmur, J., & Doty, P. (1962) *J. Mol. Biol. 5*, 109–118.

Patel, D. J., & Canuel, L. L. (1976) *Proc. Natl. Acad. Sci. U.S.A. 73*, 3343–3347.

Redfield, A. G., & Kunz, S. D. (1975) *J. Magn. Reson. 19*, 114–117.

Schweizer, M. P., Chan, S. I., Helmkamp, G. K., & T'so, P. O. P. (1964) *J. Am. Chem. Soc. 86*, 696.

Tsai, C. C., Jain, S. C., & Sobell, H. M. (1975) *Proc Natl. Acad. Sci. U.S.A. 72*, 628–632.

Tsai, C., Jain, S. C., & Sobell, H. M. (1977) *J. Mol. Biol. 114*, 301–315.

Wahl, P. L., Paoletti, C., & LePecq, J. B. (1970) *Proc. Natl. Acad. Sci. U.S.A. 65*, 417.

Woessner, E. D. (1962) *J. Chem. Phys. 37*, 647–654.

Primary Structure of AUA-Specific Isoleucine Transfer Ribonucleic Acid from *Escherichia coli*†

Yoshiyuki Kuchino, Shigeaki Watanabe, Fumio Harada, and Susumu Nishimura*

ABSTRACT: The nucleotide sequence of an *E. coli* isoleucine tRNA ($tRNA^{Ile}_{minor}$) specific for the codon AUA was determined by postlabeling procedures using only 2.5 μg (0.05 A_{260} unit) of the material. The sequence was pG-G-C-C-C-C-U-s^4U-A-G-C-U-C-A-G-U-Gm-G-D-D-A-G-A-G-C-A-A-G-C-G-A-C-U-N^+-A-U-t^6A-A-Ψ-C-G-C-U-U-G-m^7G-acp^{3}U-C-G-C-U-G-G-T-Ψ-C-A-A-G-U-C-C-A-G-C-A-G-G-G-G-C-C-A-C-C-A_{OH}. The nucleotide sequences in the regions of the D arm and TΨC arm of $tRNA^{Ile}_{minor}$ were quite similar to the corresponding regions of $tRNA^{Ile}_{major}$. However, the sequences in the CCA stem and anticodon stem of $tRNA^{Ile}_{minor}$ were different from those of $tRNA^{Ile}_{major}$. The overall homology between the two isoleucine tRNAs was 68%. *E. coli* $tRNA^{Lys}$, $tRNA^{Met}$, $tRNA^{Val}_{IIA}$ and $tRNA^{Arg}$ also have relatively high sequence homology with $tRNA^{Ile}_{minor}$.

In *Eschericia coli*, there are two isoleucine tRNA species, $tRNA^{Ile}_{major}$ and $tRNA^{Ile}_{minor}$ (Yarus & Barrell, 1971; Harada & Nishimura, 1974). The major species of $tRNA^{Ile}$ ($tRNA^{Ile}_{major}$) with guanosine in the first position of the anticodon recognizes A-U-U and A-U-C, while the minor species of $tRNA^{Ile}$ ($tRNA^{Ile}_{minor}$) recognizes only A-U-A (Harada & Nishimura, 1974). This $tRNA^{Ile}_{minor}$ contains an unknown modified nucleoside N^+ in the first position of the anticodon, which is responsible for specific recognition of the AUA codon (Harada & Nishimura, 1974).

Although the partial primary structure of $tRNA^{Ile}_{minor}$ is known (Harada & Nishimura, 1974), elucidation of the total primary structure was hampered by the difficulty of obtaining

† From the Biology Division, National Cancer Center Research Institute, Tsukiji 5-1, Chuo-ku, Tokyo, Japan. *Received October 3, 1979.*

0006-2960/80/0419-2085$01.00/0